WEP Warwick Evans Publishing

International Journal of Computer Science and Information Technology

ISSN: 3005-9682 (Print), ISSN: 3005-7140 (Online) | Volume 8, Number 1, Year 2026
DOI: https://doi.org/10.62051/ijcsit.v8n1.15
Journal homepage: https://wepub.org/index.php/IJCSIT/index

Multi-objective Magnetic Circuit Optimization of Coreless Motors Based on an Improved NSGA-Ⅲ

Wenyu Shi [1], Zhongmin Wang [1,*], Hua Zhang [2]

[1] School of Mechanical Engineering, Tianjin University of Technology and Education, Tianjin 300222, China

[2] Tianjin Institute of Aerospace Mechanical and Electrical Equipment, Tianjin 300458, China

ABSTRACT

Aiming at the problems that multi-objective optimization algorithms are prone to fall into local optima and yield uneven solution set distributions in the magnetic circuit optimization of permanent magnet DC coreless motors for the aerospace field, an improved NSGA-Ⅲ multi-objective optimization algorithm is proposed. This algorithm incorporates a dynamic adaptive crossover and mutation mechanism, a normal distribution crossover operator, and a dynamic crowding degree operator, which effectively enhances the global search capability in high-dimensional objective spaces and the distribution uniformity of the Pareto solution set, thus solving the problems that traditional algorithms tend to fall into local optima and suffer from insufficient solution set diversity in multi-objective collaborative optimization. Taking the maximization of torque coefficient, minimization of torque ripple, and minimization of magnetic leakage coefficient of the coreless motor as the core optimization objectives, a high-precision surrogate model between the objective functions and decision variables was established based on the response surface methodology, and embedded into the improved NSGA-Ⅲ algorithm to realize the multi-objective optimization of magnetic circuit parameters. Simulation results show that after optimization, the motor torque coefficient is increased by 29%, the torque ripple is reduced by 13%, and the magnetic leakage coefficient is decreased by 37%, with comprehensive performance indicators improved significantly, indicating favorable engineering application value.

KEYWORDS

Coreless Motor; Magnetic Circuit Optimization; Improved NSGA-Ⅲ; Multi-objective Optimization

1. INTRODUCTION

As a type of micro special motor with a coreless rotor structure, the permanent magnet DC coreless motor has become a core actuator in aerospace steering gear systems due to its unique structural advantages [1]. This motor type completely eliminates the hysteresis loss and eddy current loss caused by the rotor core, thus significantly improving motor energy efficiency and control sensitivity. Its low moment of inertia can meet the dynamic operating requirements of steering gear systems, such as frequent start-stop and rapid commutation, enabling delay-free response and ensuring the accuracy and timeliness of aircraft attitude adjustment. The low vibration and low noise advantages brought by the coreless structure enhance the operational stability of the steering gear system under extreme environments, effectively avoiding component wear or performance degradation caused by vibration in traditional motors. However, its special coreless structure also leads to increased magnetic circuit reluctance and obvious magnetic leakage, which in turn affects the stability of torque output and energy conversion efficiency [2]. Traditional magnetic circuit optimization methods for motors

mostly rely on engineering experience-based trial-and-error or single-objective optimization approaches, which are difficult to systematically address the trade-off between multiple conflicting objectives [3]. Therefore, it is necessary to introduce efficient multi-objective optimization methods to improve the comprehensive performance of motors.

At present, mainstream algorithms in the research of motor multi-objective optimization [4-6] include the Non-dominated Sorting Genetic Algorithm II (NSGA-II), the Multi-Objective Particle Swarm Optimization (MOPSO), and the Multi-Objective Evolutionary Algorithm based on Decomposition (MOEA/D). Benefiting from their mature principles and easy implementation, these algorithms have been widely applied to parameter optimization of general industrial motors, covering medium and low-dimensional optimization scenarios with no more than three objectives. Among them, MOPSO has weak global search capability and is prone to falling into local optima, often resulting in insufficient diversity of solution sets and failure to cover schemes with different performance trade-offs. MOEA/D decomposes multi-objective problems relying on weight vectors; its decomposition accuracy decreases significantly in the case of strong nonlinear coupling. When the number of optimization objectives exceeds four, it is difficult to achieve uniform distribution of weight vectors, leading to insufficient coverage of optimal solutions. The core limitation of NSGA-II [7] lies in high-dimensional objective scenarios. With the increase in the number of motor optimization objectives, the proportion of non-dominated solutions in the population rises sharply, making it difficult to effectively distinguish the quality of solutions. Meanwhile, the calculation of crowding distance loses effective discriminability in high-dimensional spaces, failing to ensure the uniformity of solution sets. As a result, the obtained optimal solutions may only cover partial objective directions and miss key performance combinations.

The Non-dominated Sorting Genetic Algorithm NSGA-III [8-9] is a multi-objective optimization algorithm proposed by Deb's team based on the improvement of NSGA-II. Its core is to address the shortcomings of NSGA-II in high-dimensional optimization scenarios. By introducing the reference point mechanism, adaptive normalization strategy, and niche selection strategy, NSGA-III is well adapted to high-dimensional objective optimization scenarios, balances the distribution of multiple solution sets in high-dimensional spaces, avoids local aggregation or regional gaps, and ultimately achieves accurate exploration of the Pareto optimal front. Nevertheless, the standard NSGA-III still has some drawbacks, such as fixed crossover and mutation parameters, limited exploration capability of genetic operators, and the tendency of niche selection to cause repeated selection of individuals. Especially in the magnetic circuit optimization of motors with multiple parameters, there is still room for improvement in its global search efficiency and convergence accuracy.

To solve the above problems, this study proposes an improved NSGA-III algorithm to enhance its applicability and performance in the multi-objective magnetic circuit optimization of coreless motors. The improvement strategies mainly include the following aspects: first, a dynamic adaptive crossover and mutation mechanism is introduced, which can be dynamically adjusted according to the characteristics of the optimization problem and the evolutionary state of the population; second, the normal distribution crossover operator is adopted to replace the traditional simulated binary crossover, improving the diversity of offspring generation and the exploration capability of the global solution space; third, a dynamic crowding degree operator is introduced to regulate the spatial distribution characteristics of the population. Taking the maximization of motor torque coefficient, the minimization of torque ripple and the minimization of magnetic leakage coefficient as the core optimization objectives, a high-precision surrogate model between the objective functions and decision variables (including motor housing inner diameter, magnet inner diameter, winding pitch and wire diameter) is established based on the response surface methodology. This model is then embedded into the improved NSGA-III algorithm to realize multi-objective optimization of magnetic circuit parameters and obtain the Pareto optimal solution set. Finally, the feasibility and engineering application value of the proposed optimization scheme are verified through finite element simulation.

2. NSGA-Ⅲ ALGORITHM AND ITS IMPROVEMENT

2.1. Basic Principles of the NSGA-Ⅲ Algorithm

NSGA-III is basically consistent with NSGA-II in the operations of population evolution initialization, parent and offspring population combination, and non-dominated sorting. Its core differences lie in the selection, crossover and mutation strategies during the offspring population generation phase. It mainly introduces hyperplane reference point construction, population adaptive normalization, the mapping relationship between population individuals and reference points, and niche preservation operations [7]. The specific implementation process is as follows:

(1) Non-dominated ranking classification serves as the basis for population screening, with its core objective being to select a candidate set of appropriate size from the merged population, so as to lay the groundwork for subsequent refined selection. If the number of individuals in the merged population S_t is exactly equal to the preset population size N, population S_t will be directly adopted as the parent population P_{t+1} of the next generation. If the size of population S_t exceeds N, a stepwise screening process based on non-dominated ranks is required. First, the non-dominated individuals of the top $t-1$ ranks are incorporated into the parent population P_{t+1} of the next generation. At this point, there are still $K = N - |P_{t+1}|$ vacancies in population P_{t+1}. Finally, it is necessary to further select K optimal individuals from the non-dominated individual set F_t of the L-th rank to supplement population P_{t+1}, thus completing the preliminary scale control.

(2) Determination of hyperplane reference points for constructing a uniform distribution in the high-dimensional space. Given the preset population size, the dimension of the objective function, and the number of partitions in the objective space, a hyperplane is constructed on the basis of reference points, and its mathematical expression is as follows:

$$H = C_{M+p-1}^{p} \tag{1}$$

(3) Adaptive normalization of the population. The normalization formula for each individual in the population is expressed as follows:

$$f_i^n(x) = \frac{f_i(x) - z_i^{min}}{\alpha_i}, \quad i = 1, 2, ..., M \tag{2}$$

Where $f_i(x)$ is the original objective value of the i-nd objective; z_i^{min} is the global minimum value of the i-th objective; α_i is the intercept of the i-th objective; $f_i^n(x)$ is the normalized objective value of the i-th objective for the n-th individual, which satisfies the condition $\sum_{i=1}^{M} f_i^n = 1$.

(4) Establishing the mapping relationship between population individuals and reference points. First, with the origin as the starting point, reference lines extending from the origin to each reference point are constructed, and all such reference lines lie on the established hyperplane. The perpendicular distance from each individual in population S_t to each reference line is calculated, and the reference point corresponding to the minimum distance is defined as the associated reference point of this individual, which ensures that the individual is highly aligned with the objective direction of the reference point.

(5) Niche preservation operation. The total number of individuals with a Pareto rank lower than N is equal to P_{t+1}, which is the total number of individuals in the top L-1 ranks. However, the total number of individuals in the top L Pareto ranks exceeds N. Hence, K individuals are to be selected from the population F_t with a Pareto rank of L, among which $K = N - P_{t+1}$.

A reference point may have no associated individuals, or be associated with one or more individuals, where p_j denotes the number of individuals associated with the j-th reference point. The niche preservation operation first counts the number of associated individuals for each reference point j, and prioritizes the set of reference points with the smallest number of associated individuals; if multiple reference points have the same number of associated individuals, one is selected randomly. The specific selection logic is as follows: if $p_j=0$, no individuals corresponding to this reference point are selected; if $p_j \geq 1$, one associated individual is randomly selected and incorporated into P_{t+1}, and the count of pj is incremented by one. The above selection process is repeated K times until the size of P_{t+1} reaches N, thus completing the entire population selection.

In summary, the population selection strategy of NSGA-III establishes reference points in the objective space and builds the mapping relationship between population individuals and these reference points, then employs niche preservation to maintain population diversity. This approach addresses the problem of uneven distribution of solution sets in high-dimensional spaces, ensures the diversity of solutions, and ultimately achieves uniform coverage of the Pareto optimal front in the objective space.

2.2. An Improved NSGA-Ⅲ Algorithm

(1) Dynamic Adaptive Adjustment

The crossover probability and mutation probability adopted in the traditional NSGA-III algorithm follow a fixed pattern. The static parameter configuration fails to adapt to the requirements of different stages in the optimization process. Specifically, the parameter settings may be overly conservative when strong exploration capability is required in the early stage of optimization, while they may turn out to be excessively radical when strong exploitation capability is needed in the later stage. This parameter rigidity is prone to cause search stagnation, making the algorithm unable to adaptively adjust its exploration and exploitation capabilities in both the early and late stages of evolution.

In this paper, an adaptive crossover and mutation mechanism is introduced. The core idea is to dynamically adjust the crossover probability and mutation probability according to the characteristics of the optimization problem and the evolutionary state of the population, instead of using fixed values. Through the dynamic adaptation of the strategy, the population is prevented from falling into local optima due to insufficient diversity in the early stage of evolution, or from experiencing a decline in convergence efficiency due to excessive randomization in the later stage. The specific setting of the probabilities is as follows:

$$G_1 = G_{1\max}\left(1 - \frac{G_{1\min}}{G_{1\max}} \times \frac{\mathrm{t}}{T}\right) \tag{3}$$

Where G_1 denotes the crossover probability; $G_{1\max}$ is the maximum crossover probability; $G_{1\min}$ is the minimum crossover probability; t represents the current number of iterations; and T is the maximum number of iterations.

$$G_2 = G_{2\max}\left(1 - \frac{G_{2\min}}{G_{2\max}} \times \frac{\mathrm{t}}{T}\right) \tag{4}$$

Where G_2 denotes the mutation probability; $G_{2\max}$ is the maximum mutation probability; and $G_{2\min}$ is the minimum mutation probability.

(2) Enhancement of Genetic Operators

The NSGA-III algorithm adopts the conventional simulated binary crossover SBX operator. During gene recombination, the generation mode of offspring individuals is relatively fixed, with limited fluctuations mainly around the gene range of parent individuals. This makes it difficult to break through the constraints of the local search space, leading to a gradual convergence of the population during the evolutionary process. Particularly in high-dimensional objective spaces or multimodal problems, such convergence will rapidly narrow the distribution range of solutions, trapping the algorithm in local optima and preventing it from exploring a broader range of potential optimal solutions.

Compared with the conventional SBX operator, the normal distribution crossover NDX operator demonstrates remarkable advantages in balancing exploration and exploitation capabilities. Centered on the mean value of parent individuals, this operator regulates the generation of offspring by virtue of the probabilistic characteristics of normal distribution, which significantly increases the probability density of offspring distributed around the parent individuals. This means that the algorithm can inherit the excellent genes of parents more efficiently, concentrate computing resources on in-depth exploitation within the known high-quality regions, and thus enhance the exploitation efficiency of the local solution space. Meanwhile, the tail characteristics of normal distribution also reserve a certain probability of generating individuals far away from the parents. These individuals can break through the current search scope, introduce new evolutionary directions for the population, and avoid falling into local optima, thereby effectively strengthening the exploration capability of the global solution space. Such a probability distribution characteristic of high density in the vicinity and low density in the distance exactly makes up for the deficiency of the SBX operator in balancing exploration and exploitation, enabling the NDX operator to better balance the convergence speed and population diversity in complex optimization problems.

An approach is proposed for the construction of the normal distribution crossover NDX operator. First, a random number z that follows a uniform distribution over the interval (0, 1) is generated. When z≤0.5:

$$\begin{cases} x_{1,i}=\dfrac{p_{1,i}+p_{2,i}}{2}+\dfrac{1.481\times\left(p_{1,i}-p_{2,i}\right)\times\left|N(0,1)\right|}{2} \\ x_{2,i}=\dfrac{p_{1,i}+p_{2,i}}{2}-\dfrac{1.481\times\left(p_{1,i}-p_{2,i}\right)\times\left|N(0,1)\right|}{2} \end{cases} \tag{5}$$

When z>0.5:

$$\begin{cases} x_{1,i}=\dfrac{p_{1,i}+p_{2,i}}{2}-\dfrac{1.481\times\left(p_{1,i}-p_{2,i}\right)\times\left|N(0,1)\right|}{2} \\ x_{2,i}=\dfrac{p_{1,i}+p_{2,i}}{2}+\dfrac{1.481\times\left(p_{1,i}-p_{2,i}\right)\times\left|N(0,1)\right|}{2} \end{cases} \tag{6}$$

Where $p_{1,i}$ and $p_{2,i}$ represent the information of Parent 1 and Parent 2 on the i rd chromosome, respectively; $x_{1,i}$ and $x_{2,i}$ denote the information of Offspring 1 and Offspring 2 on the i-th chromosome, respectively; and $\left|N(0,1)\right|$ is a standard normal distribution random variable. Specifically, through the designed specific chromosome information transmission rules and random variable settings, the NDX crossover operator achieves effective inheritance of parental genes to

offspring, thus demonstrating significantly superior search capability compared with the conventional SBX crossover operator.

(3) Dynamic Crowding Degree Operator

In the reference-point-based niche selection process of the NSGA-III algorithm, when the niche individual count of a certain reference point is relatively small, the problem of excessive individual selection is prone to occur, which in turn exerts a negative impact on population evolution. Before the niche selection completes K iteration, the individuals associated with the reference points with small niche counts are likely to be repeatedly selected into the next-generation population S_t. The core reason is that although the niche count of the reference point is incremented by one each time an individual is selected from it, the updated count remains at a low level due to its initial count being far lower than that of other reference points. Thus, such reference points still become the priority candidates in the subsequent selection rule of priority to the minimum niche count. This phenomenon of continuously selecting individuals from the same reference point leads to two major drawbacks: first, it undermines population diversity, causing the population to be excessively concentrated in the objective region corresponding to this reference point while making it difficult for individuals in other regions to enter the next generation; second, it slows down the population convergence speed. Repeatedly selecting individuals with similar characteristics leads to the simplification of population evolution directions, hindering the rapid approximation to the Pareto optimal front and reducing the overall optimization efficiency.

In this paper, a dynamic crowding distance operator is introduced, which actively regulates the spatial distribution characteristics of the population by adding a crowding distance judgment in the individual screening process. The core operation of this operator is embedded before the process of selecting individuals from the reference-point-associated set into the next generation. For all individuals associated with a specific reference point, the crowding distance between any two individuals in the set is first calculated. The obtained crowding distance is then compared with a preset threshold. If the crowding distance between two individuals is less than this threshold, one of them is randomly eliminated, so that the eliminated individual will not participate in the subsequent screening and evolution processes of the next-generation population. The calculation formula of its dynamic crowding distance is as follows:

$$D = \sqrt{\sum_{i=1}^{m} \left(\left| f_i(x_1) - f_i(x_2) \right|^2 \right)} \tag{7}$$

Where x_1 and x_2 are two population members; $f_i(x_1)$ is the original objective value of the i-th objective for individual x_1; and $f_i(x_2)$ is the original objective value of the i-th objective for individual x_2.

2.3. Algorithm Performance Verification

In the performance verification of multi-objective optimization algorithms, the ZDT series and DTLZ series of functions are two types of widely recognized standard test functions [10]. Their covered objective dimensions and front characteristics can effectively verify the adaptability of the algorithms. To comprehensively evaluate the optimization performance of the improved algorithm proposed in this paper, these two types of functions are selected in a targeted manner to construct test scenarios. In the dual-objective optimization scenario, three functions including ZDT1, ZDT2 and ZDT3 from the ZDT series are adopted. The Pareto fronts of these functions correspond to convex, non-convex and discrete characteristics respectively, which can verify the search and convergence performance of the improved algorithm in different dual-objective spaces. In the tri-objective optimization scenario, the DTLZ2 function from the DTLZ series is selected. The high-dimensional objective characteristics

and continuous Pareto front of this function can further verify the exploration capability of the improved algorithm in complex solution spaces and the control effect of solution set distribution when the objective dimension is increased.

As illustrated in Figs. 1–4, under the condition of the same number of iterations, the Pareto front curves generated by the improved NSGA-III algorithm demonstrate significantly better approximation to the true Pareto front than those generated by the traditional NSGA-III algorithm. In terms of the breadth of solution set coverage, the improved algorithm exhibits a marked improvement in the solution set performance across all objective dimensions, specifically reflected in more uniform coverage of the solution space and the avoidance of solution set vacancies in local regions. Meanwhile, the solution set shows a higher aggregation density in key regions, achieving in-depth exploitation of high-quality solution spaces. In summary, during the iterative process of the test functions, the improved NSGA-III algorithm simultaneously enhances the convergence accuracy and solution set diversity. The optimization effects of both aspects verify the effectiveness of the improvement strategies proposed in this study for boosting the search performance of the algorithm.

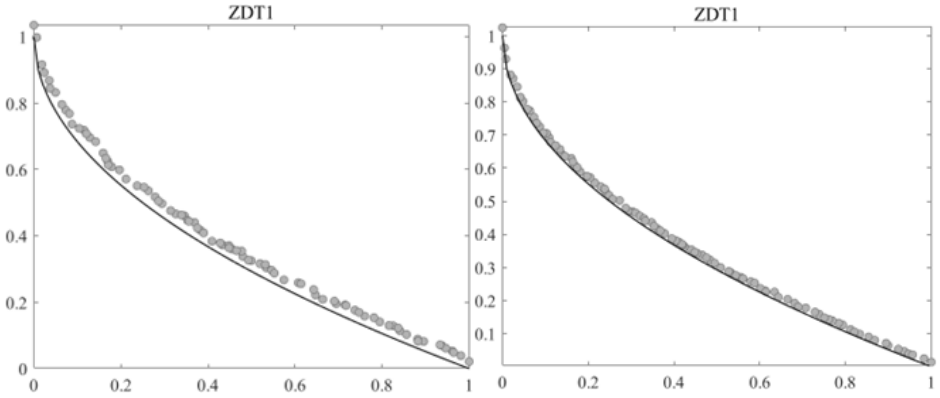

(a) NSGA-III (b) Improved NSGA-III

Figure 1. Fitting Curves of Pareto Fronts of NSGA-III Algorithms Before and After Improvement on ZDT1

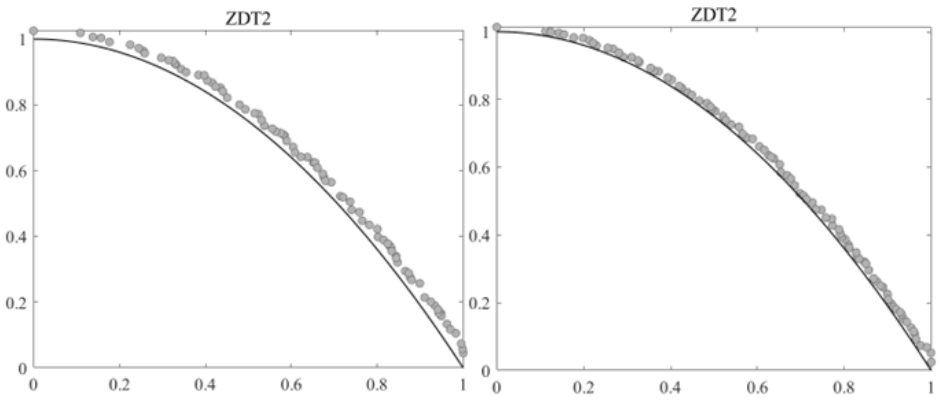

(a) NSGA-III (b) Improved NSGA-III

Figure 2. Fitting Curves of Pareto Fronts of NSGA-III Algorithms Before and After Improvement on ZDT2

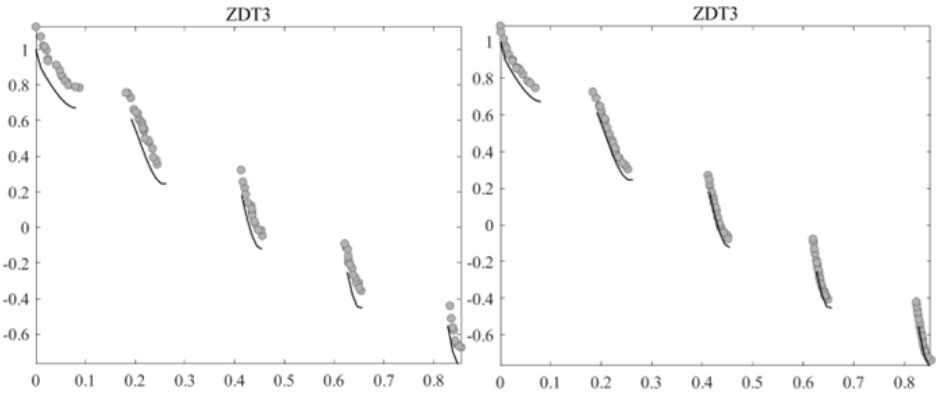

(a) NSGA-III (b) Improved NSGA-III

Figure 3. Fitting Curves of Pareto Fronts of NSGA-III Algorithms Before and After Improvement on ZDT3

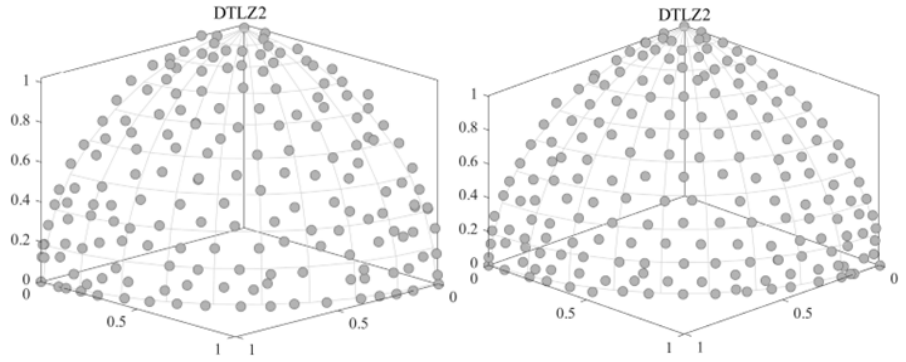

(a) NSGA-III (b) Improved NSGA-III

Figure 4. Fitting Surfaces of Pareto Fronts of NSGA-III Algorithms Before and After Improvement on DTLZ2

Based on the comprehensive test results of the ZDT1, ZDT2 and ZDT3 dual-objective functions as well as the DTLZ2 tri-objective function, the improved NSGA-III algorithm is significantly superior to the original traditional algorithm in terms of convergence and solution set distribution uniformity. In the tests on ZDT1-ZDT2-ZDT3 functions, the Pareto front curves generated by the improved algorithm have a higher degree of fitting with the true Pareto fronts, and can more accurately conform to the distribution trend of the theoretical optimal solutions. In the three-dimensional test scenario of the DTLZ2 function, the solution set of the traditional algorithm not only has an obvious gap from the spherical surface of the true Pareto front, but also deviates from the spherical distribution in some regions. In contrast, the solution set of the improved algorithm is not only more uniformly distributed over the entire spherical front without local aggregation or sparsity, but also closely adheres to the true spherical surface as a whole. These results fully verify the effectiveness of the proposed improvement strategies in enhancing the high-dimensional optimization capability of the algorithm.

3. MULTI-OBJECTIVE MAGNETIC CIRCUIT OPTIMIZATION

3.1. Construction of Optimization Model Equations

(1) Optimization Objectives and Variables

The core feature that distinguishes the permanent magnet DC brushless coreless motor from traditional motors lies in its coreless structure. Although this structure offers the advantage of cogging torque elimination, it also leads to shortcomings in magnetic circuit performance. Especially in

aerospace applications, there is a demand to balance high driving capability, high torque smoothness, and high magnetic energy utilization within a limited volume. Therefore, the establishment of magnetic circuit optimization objectives must be closely integrated with structural characteristics and application requirements. In this paper, the optimization objectives are defined as maximizing the torque coefficient under rated load, minimizing torque ripple, and minimizing the magnetic leakage coefficient.

Combined with the theoretical structural parameters of the motor, the relevant variables of the objective function are defined. The motor design dimensions and the value ranges of the variables are shown in Table 1.

Table 1. Motor Design Dimensions and Variable Value Ranges

variables	Name	Design dimensions	Variable range
x_1	Inner diameter of the casing	18mm	17.5-18.5mm
x_2	Magnet outer diameter	14mm	13-15mm
x_3	Magnet inner diameter	5mm	4-6mm
x_4	Magnet axial length	19mm	18-20mm
x_5	Axial length of the casing	25mm	24-26mm
x_6	Winding inner diameter	15mm	14.5-15.5mm
x_7	Winding outer diameter	17mm	16.5-17.5mm
x_8	Winding pitch	25.13mm	24.32-25.92mm
x_9	Winding axial length	24mm	23.5-24.5mm
x_{10}	Arc coefficient	065	0.65-0.90
x_{11}	Conductor diameter	0.117mm	0.085-0.158mm
x_{12}	Total number of winding turns	300	200-1000

(2) Construction of the Optimization Model

Based on the sensitivity analysis with Latin hypercube sampling [11], three key indicators, namely torque coefficient K_T, torque ripple T_r, and magnetic leakage coefficient λ, were calculated for the sampling points. A threshold of 0.17 was set as the criterion for the comprehensive sensitivity of each design variable, and the inner diameter of the motor housing, inner diameter of the magnet, winding pitch, and wire diameter were selected as decision variables for multi-objective optimization. The central composite design (CCD) was adopted to generate sampling points, with 5 repetitions at the central point, resulting in a total of 30 groups of basic experiments. Corresponding torque coefficients, torque ripples, and magnetic leakage coefficients were obtained via Ansys Maxwell finite element simulation. The experimental data were analyzed using Design-Expert software, and a response surface model was established based on statistical principles [12]. Through regression analysis of the simulation results, a polynomial function was used to map the relationship between the optimization variables and optimization objectives, thus deriving the corresponding response surface model. For this experiment, a quadratic regression equation was employed for fitting calculation, and the specific mathematical model is as follows:

$$F(x) = \beta_0 + \sum_{i=1}^{m} \beta_i x_i + \sum_{i=1}^{m} \beta_{ii} x_i^2 + \sum_{i=1}^{m} \sum_{j=1, j \neq i}^{m} \beta_{ij} x_i x_j + \varepsilon \tag{8}$$

Where $F(x)$ is the objective value, β_0 is the regression coefficient of the model, m is the number of variables, $\beta_i x_i$ is the linear term, $\beta_{ii} x_i^2$ is the quadratic term, $\beta_{ij} x_i x_j$ is the interaction term, and ε is the error term.

Three second-order response surface equations are obtained after collation, namely the response surface model equation for torque coefficient:

$$K_T = +5.78 - 0.1308x_1 - 0.1933x_3 - 0.1875x_8 + 2.83x_{11} + 0.0263x_1x_8 - 0.0562x_1x_{11} \\ +0.0088x_3x_8 - 0.0962x_3x_{11} - 0.08x_8x_{11} - 0.0669x_1^2 - 0.0931x_3^2 - 0.0506x_8^2 + 0.0919x_{11}^2 \quad (9)$$

The response surface model equation for torque ripple:

$$T_r = +67 - 0.7917x_1 - 1.13x_3 + 1.12x_8 - 9.13x_{11} + 0.1875x_1x_3 - 0.1875x_1x_8 + 0.1875x_1x_{11} \\ -0.0625x_3x_8 + 0.3125x_3x_{11} - 0.3125x_8x_{11} - 0.3021x_1^2 - 0.1771x_3^2 + 0.0729x_8^2 + 1.32x_{11}^2 \quad (10)$$

And the response surface model equation for magnetic leakage coefficient:

$$\lambda = +1.09 + 0.016x_1 - 0.0062x_3 - 0.0059x_8 - 0.0011x_1x_3 - 0.005x_1x_8 + 0.0006x_3x_8 \\ +0.001x_1^2 + 0.0006x_3^2 + 0.0009x_8^2 + 0.0008x_{11}^2 \quad (11)$$

Where x_1, x_3, x_8, and x_{11} are the inner diameter of the motor housing, inner diameter of the magnet, winding pitch, and wire diameter, respectively.

3.2. Optimization Based on the Improved NSGA-Ⅲ

The flowchart for multi-objective optimization of the magnetic circuit parameters of coreless motors using the improved NSGA-III algorithm is shown in Fig. 5. First, based on the initialization of the parent population, the optimization objectives, variables, and surrogate model are defined. Second, the adaptive crossover and mutation mechanism is introduced in the selection, crossover, and mutation phases; meanwhile, the normal distribution crossover NDX operator is adopted to generate the offspring population. The dynamic crowding degree operator is incorporated into the niche selection and calculation of reference points, thus ultimately achieving the multi-objective optimization of the magnetic circuit parameters.

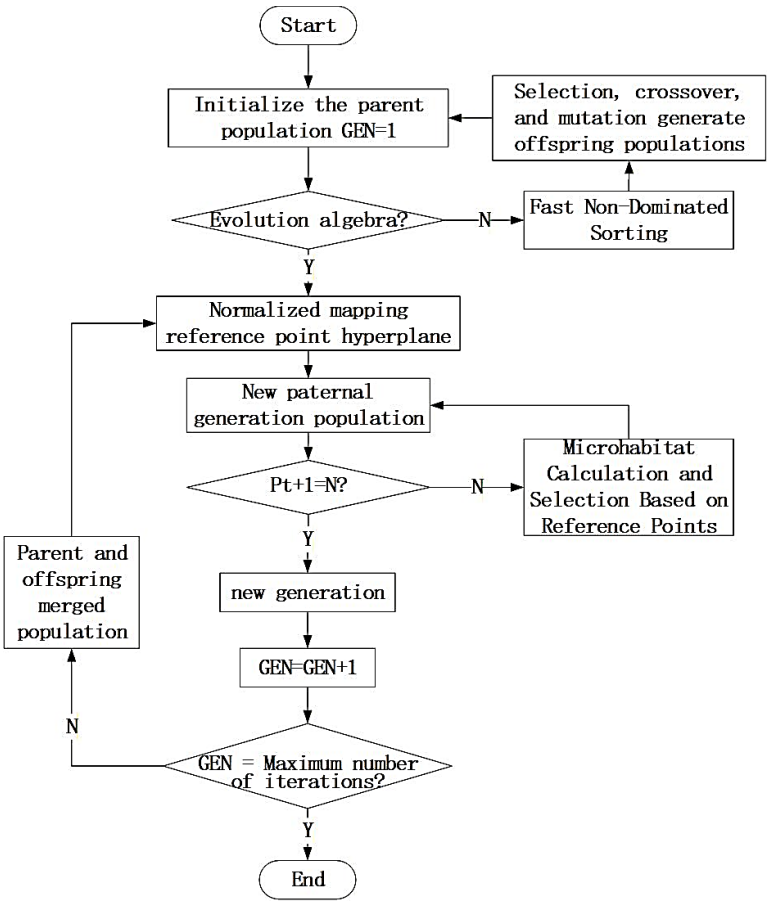

Figure 5. Flowchart of the Improved NSGA-III Algorithm Optimization

The algorithm is configured with a population size of 91, a maximum number of iterations of 100, 4 optimization decision variables, and 3 optimization objectives. The simulation analysis and iterative solution are completed on the MATLAB platform, and the final Pareto optimal front solution set corresponding to the fitness function is obtained, as shown in Fig. 6.

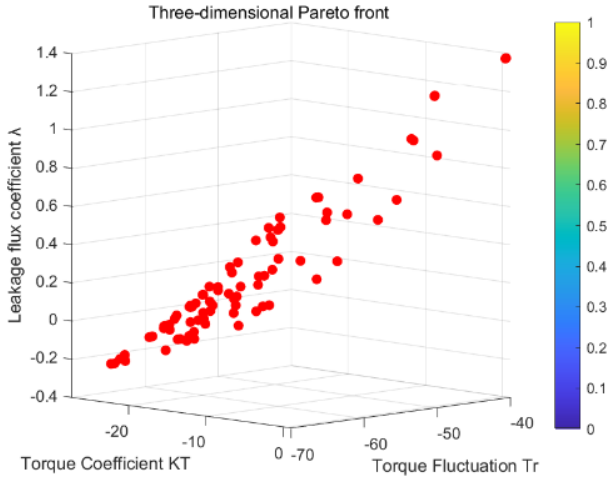

Figure 6. Pareto frontier chart

When the Improved NSGA-III algorithm is applied to solve such multi-objective optimization problems, it generates a set of Pareto optimal solution sets satisfying the non-dominated property after each iteration, rather than directly outputting a unique global optimal solution as in single-objective optimization. Therefore, after the algorithm runs to the maximum number of iterations, the corresponding optimal decision variable values and the optimized values of each objective function are determined through trade-off analysis, as shown in Table 2.

Table 2. Optimized variables and target values

decision variable	value	Optimization Goal	Value
Inner diameter of the casing	18.2mm	moment coefficient	5.97
Magnet inner diameter	4mm	Torque fluctuation	53.15%
Winding pitch	25.29mm	Magnetic leakage coefficient	1.05
Conductor diameter	0.094mm		

4. SIMULATION EXPERIMENT AND DISCUSSION

4.1. Simulation Experiment Results

To verify the magnetic circuit optimization effect based on the Improved NSGA-III algorithm, a three-dimensional finite element simulation model of the permanent magnet DC coreless motor was established on the Ansys Maxwell platform. The model adopted a transient magnetic field solver, with copper as the winding material, N52H neodymium iron boron as the permanent magnet material, and DT4C pure iron as the motor housing material. The balloon boundary was selected as the boundary condition, and the mesh was locally refined in the air gap and winding regions to balance the calculation accuracy and efficiency.

Under the rated operating conditions (24V, 3800r/min), a simulation comparison was conducted on the motor before and after optimization. The initially designed parameters were adopted for the motor prior to optimization, while the values of decision variables shown in Table 2 were selected for the optimized motor. Identical simulation conditions and boundary settings were applied to eliminate external interference.

The simulation results are shown in Table 3. After optimization, the torque coefficient increased from 5.78mNm/A to 5.95mNm/A, with an increase of approximately 29%; the torque ripple decreased from 67% to 58%, with a reduction of approximately 13%; the magnetic leakage coefficient decreased from 1.09 to 1.05, with a reduction of approximately 37%.

Table 3. Comparison of Optimization Goals

Parameter Name	Before	After
moment coefficient	5.78mNm/A	5.95mNm/A
Torque fluctuation	67%	58%
Magnetic leakage coefficient	1.09	1.05

Furthermore, a further observation from the comparison curves in Figs. 7 indicates that: although the peak electromagnetic torque decreases from 11.90mNm to 7.91mNm after optimization, the fluctuation range is significantly reduced, which means that the motor output is more stable and conducive to reducing vibration and noise; the peak current is obviously suppressed, dropping from 2.06A to 1.33A, thus lowering the system control load; the winding copper loss decreases from 2.86W to 1.18W, with a reduction of 38.3%, which directly reflects the inhibitory effect of wire diameter and winding layout optimization on resistance loss and helps reduce temperature rise; the harmonic content of the air-gap magnetic density curve is reduced and the distribution tends to be more uniform, demonstrating that the magnetic circuit design effectively suppresses magnetic leakage and local saturation.

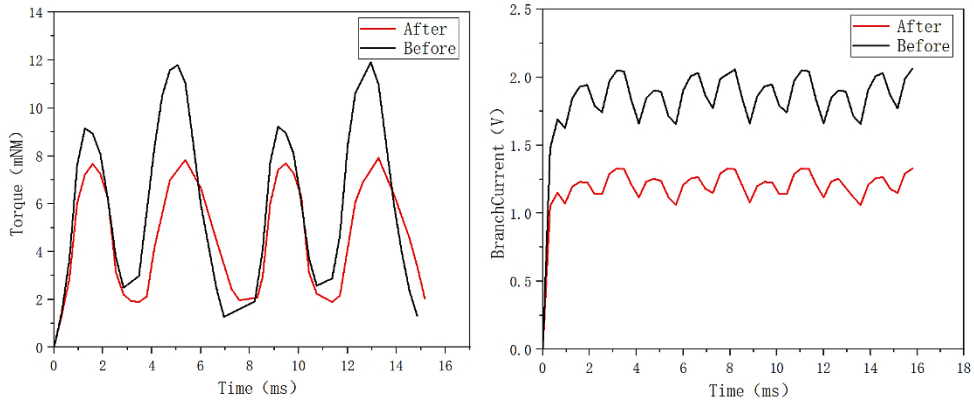

(a) Electromagnetic torque (b) Drive current

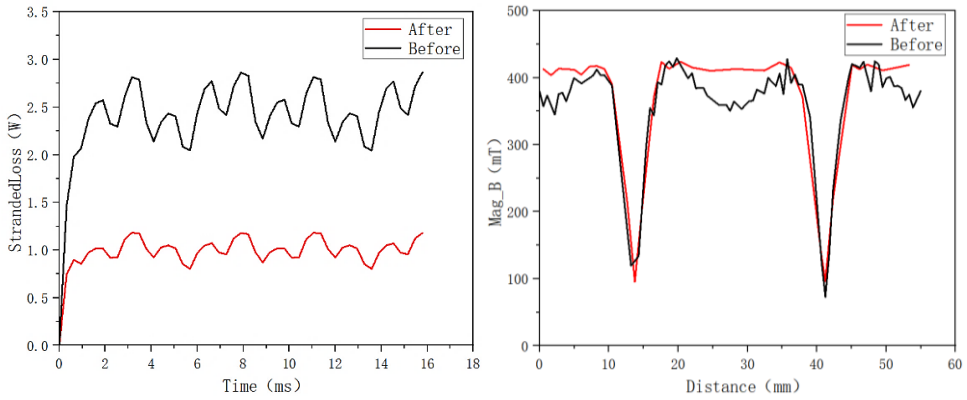

(c) Winding Loss (d) Air gap magnetic flux density

Figure 7. Comparison curves of motor parameters before and after optimization

Table 4 further summarizes the comprehensive performance comparison under load conditions, where the motor efficiency is increased from 89% to 93%, verifying the effectiveness of the optimization measures in improving the energy conversion efficiency.

Table 4. Comparison of Main Parameters for Motor Simulation

Parameter Name	Before	After
Electromagnetic torque	11.90mNm	7.91mNm
Drive current	2.06A	1.33A
Winding Loss	2.86W	1.18W
Efficiency	89%	93%

In summary, this study adopts the improved NSGA-III algorithm to complete the multi-objective optimization of the magnetic circuit of the coreless motor, which effectively enhances the air-gap magnetic density, improves the uniformity of magnetic circuit distribution, reduces magnetic density distortion, and achieves the comprehensive improvement of the motor's core performance.

4.2. Discussion

Aiming at the limitations of the traditional NSGA-III algorithm in the high-dimensional optimization of motor magnetic circuits, namely fixed crossover and mutation parameters, unbalanced exploration and exploitation of genetic operators, and individual redundancy in niche selection, this study proposes a triple improvement strategy consisting of a dynamic adaptive crossover and mutation mechanism, a normal distribution crossover NDX operator, and a dynamic crowding degree operator. This strategy achieves a balance between the global exploration and local exploitation of the

algorithm and improves the uniformity and diversity of the solution set. Verified by the ZDT and DTLZ2 test functions, the improved algorithm exhibits a significantly higher fitting degree of the Pareto front, with gap-free solution set coverage in dual-objective scenarios and more uniform distribution in high-dimensional scenarios. These results demonstrate the effectiveness of the improvement strategy in enhancing the algorithm's convergence accuracy and solution set diversity, providing reliable support for the multi-objective optimization of motor magnetic circuits.

Based on the three-dimensional finite element simulation model established in Ansys Maxwell, the motor performance indicators before and after optimization were compared under rated operating conditions, which verified the engineering value of the improved algorithm. After optimization, the motor torque coefficient is increased by 29%, indicating that the optimization of magnetic circuit structural parameters effectively reduces the magnetic resistance of the main magnetic flux path and improves the conversion efficiency; the torque ripple is reduced by 13%, which shows that the optimization of winding pitch and wire diameter suppresses end magnetic leakage and magnetic density distortion, thus improving output stability; the magnetic leakage coefficient is reduced by 37%, reflecting that parameter matching optimizes the magnetic flux path, reduces magnetic energy loss, and improves the utilization rate of permanent magnets. In addition, the motor driving current is reduced by 35%, and the winding copper loss is reduced by 38.3%, which reflects the inhibitory effect of wire diameter optimization on resistance loss; the motor efficiency is increased to 93%, achieving an improvement in energy conversion efficiency and providing a guarantee for the operation of the motor under extreme aerospace conditions.

In summary, the improved NSGA-III algorithm enhances the accuracy and effectiveness of multi-objective optimization through mechanism innovation. The dynamic adaptive crossover and mutation mechanism strengthens the algorithm's global search capability in the high-dimensional objective space of motor magnetic circuits, ensuring that the algorithm breaks through the local optimal trap and explores the optimal matching combination of key parameters; the NDX operator's ability to balance global exploration and local exploitation enables the algorithm to accurately capture the optimal parameter values and achieve comprehensive performance improvement; the uniform solution set characteristic of the dynamic crowding degree operator allows the algorithm to find the optimal trade-off point among multiple conflicting objectives. The magnetic circuit parameters obtained by the optimization improve the magnetic circuit characteristics of the coreless motor, providing a feasible optimization scheme for the motors used in aerospace actuator systems.

5. CONCLUSION

Aiming at the problems that traditional algorithms are prone to fall into local optima and generate uneven solution sets in the multi-objective optimization of magnetic circuits for permanent magnet DC coreless motors in the aerospace field, this paper proposes an improved NSGA-III algorithm integrated with a dynamic adaptive crossover and mutation mechanism, a normal distribution crossover NDX operator, and a dynamic crowding degree operator. Verified by the ZDT series and DTLZ2 test functions, the algorithm exhibits significantly superior high-dimensional space search capability and Pareto solution set uniformity compared with the traditional NSGA-III. Taking the maximization of torque coefficient and the minimization of torque ripple as well as magnetic leakage coefficient as the optimization objectives, combined with the decision variables screened via sensitivity analysis, a high-precision surrogate model established based on the response surface methodology was embedded into the improved algorithm for optimization. Ansys Maxwell simulation results show that after optimization, the motor torque coefficient is increased by 29%, the torque ripple is reduced by 13%, and the magnetic leakage coefficient is decreased by 37%. Meanwhile, the motor current, copper loss and efficiency are improved synchronously, providing a high-performance optimization scheme for aerospace actuator systems.

ACKNOWLEDGEMENTS

This research was funded by the Tianjin Education Commission Research Program Project [Project No. 2022ZD027], the Tianjin.

REFERENCES

[1] Xu Chenqi, Zhu Changsheng. A Magnetic-Structural Bidirectional Coupling Analysis Method for Electromagnetic Vibration of Electrical Machines Based on Quasi-3D Electromagnetic Field Model [J]. Proceedings of the CSEE, 2025, (05): 1922-1935.

[2] Song Wenjie, Liu Yansong, Xing Hailong, et al. Influence of Winding Configuration on the Power of Coreless Motors [J]. Journal of Ordnance Equipment Engineering, 2024, 45(09): 58-64+94.

[3] Li Fan, Gao Liang, Shen Weiming. Surrogate-Assisted Multi-Objective Evolutionary Optimization With Pareto Front Model-Based Local Search Method [J]. IEEE Transactions on Cybernetics, 2024, 54(1): 173-186.

[4] Bushra Alhijawi, Arafat Awajan. Genetic algorithms: theory, genetic operators, solutions, and applications [J]. Evolutionary Intelligence, 2024, 17(3): 1245-1256.

[5] Chunyuan Liu, Rui Dong, Baolin Ye. Comprehensive Sensitivity Analysis and Multi-Objective Optimization on a Permanent Magnet Linear Generator for Wave Energy Conversion [J]. Ssrn Electronic Journal, 2021.

[6] Liu Feng, Wang Xiuhe, Wei Hongye. Fast Magnetic Field Prediction Based on Hybrid Subdomain Method and Multiobjective Optimization Design for Interior Permanent Magnet Synchronous Machines [J]. IEEE Transactions on Energy Conversion, 2023, 38(3): 2045-2060.

[7] Bushra Alhijawi, Arafat Awajan. Genetic algorithms: theory, genetic operators, solutions, and applications [J]. Evolutionary Intelligence, 2024, 17(3): 1245-1256.

[8] Hernandez C, Lara J, Arjona M.-A, et al. Electromagnetic Optimal Design of a PMSG Considering Three Objectives and Using NSGA-III [J]. IEEE Transactions on Magnetics, 2022, 58(9): 1-4.

[9] Wang Weinan, Wang Shuo, Zhao Xiaokun, et al. Multi-Objective Optimization of Asymmetric PM-Assisted Synchronous Reluctance Motor Based on NSGA-III [C]//2024 IEEE 7th International Electrical and Energy Conference (CIEEC): IEEE, 2024: 4946-4951.

[10] Wang Liping, Ren Yu, Qiu Qicang, et al. A Survey on Performance Indicators for Multi-Objective Evolutionary Algorithms [J]. Chinese Journal of Computers, 2021, 44(08): 1590-1619.

[11] Ioannis Iordanis, Christos Koukouvinos, Iliana Silou. On the efficacy of conditioned and progressive Latin hypercube sampling in supervised machine learning [J]. Applied Numerical Mathematics, 2025, 208: 256-270.

[12] Zhao Wenxiang, Ma Anqi, Ji Jinghua, et al. Multiobjective Optimization of a Double-Side Linear Vernier PM Motor Using Response Surface Method and Differential Evolution [J]. IEEE Transactions on Industrial Electronics, 2020, 67(1): 80-90.